The Optimization of 3.3 kV 4H-SiC JBS Diodes

Arne Benjamin Renz, *Student Member, IEEE*, Vishal Ajit Shah, Oliver James Vavasour, Guy William Clarke Baker, *Student Member, IEEE*, Yegi Bonyadi, Yogesh Sharma, Vasantha Pathirana, Tanya Trajkovic, *Member, IEEE*, Phil Mawby, *Senior Member, IEEE*, Marina Antoniou, and Peter Michael Gammon, *Senior Member, IEEE*

***Abstract*— The article reports a comprehensive study optimizing the OFF- and ON-state characteristics of 3.3 kV junction barrier Schottky (JBS) diodes made using nickel, titanium, and molybdenum contact metals. In this design, the same implants used in the optimized termination region are used to form the P-regions in the JBS active area. The width and spacing of the P-regions are varied to optimize both the ON- and OFF-state of the device. All the diodes tested displayed high blocking voltages and ideal turn-on characteristics up to the rated current of 2 A. However, the leakage current and the Schottky barrier height (SBH) were found to scale with the ratio of Schottky to p$^+$ regions. Full Schottkys, without p$^+$ regions, and those with very wide Schottky regions had the lowest SBH (1.61 eV for Ni, 1.11 eV for Mo, and 0.87 eV for Ti) and the highest leakage. Those diodes with the lowest Schottky openings of 2 μm had the lowest OFF-state leakage, but they suffered severe pinching from the surrounding p$^+$ regions, increasing their SBH. The best performing JBS diodes were Ni and Mo devices with the narrowest pitch, with the p$^+$ implants/Schottky regions both 2 μm wide. These offered the best balanced device design, with excellent OFF-state performance, while the Schottky ratio guaranteed a relatively low forward voltage drop.**

***Index Terms*— JBS diodes, Mo, Ni, Schottky diodes, silicon carbide, termination design, Ti.**

I. Introduction

RECENT progress in growth and processing technology has made wide bandgap semiconductor materials realistic

Manuscript received September 25, 2021; revised November 1, 2021; accepted November 17, 2021. Date of publication December 2, 2021; date of current version December 29, 2021. This work was supported in part by the Engineering and Physical Science Research Council (EPSRC) under Grant EP/R00448X/1 and in part by the Innovate U.K. funded TRASiCA Project under Grant 102897. The review of this article was arranged by Editor M. Hua. *(Corresponding author: Arne Benjamin Renz.)*

Arne Benjamin Renz, Vishal Ajit Shah, Oliver James Vavasour, Guy William Clarke Baker, Phil Mawby, Marina Antoniou, and Peter Michael Gammon are with the School of Engineering, University of Warwick, Coventry CV4 7AL, U.K. (e-mail: a.renz@warwick.ac.uk; vishal.shah@warwick.ac.uk; guy.baker@warwick.ac.uk; p.a.mawby@warwick.ac.uk; marina.antoniou@warwick.ac.uk; p.m.gammon@warwick.ac.uk).

Yegi Bonyadi is with Lyra Electronics Ltd., Wellesbourne CV35 9EF, U.K. (e-mail: ybonyadi@lyraelectronics.com).

Yogesh Sharma is with Bosch AG, 72762 Reutlingen, Germany (e-mail: yogesh.sharma3@de.bosch.com).

Vasantha Pathirana and Tanya Trajkovic are with Cambridge Microelectronics Ltd., Cambridge CV23 6DP, U.K. (e-mail: vasantha.pathirana@warwick.ac.uk; tanya.trajkovic@warwick.ac.uk).

Color versions of one or more figures in this article are available at https://doi.org/10.1109/TED.2021.3129705.

Digital Object Identifier 10.1109/TED.2021.3129705

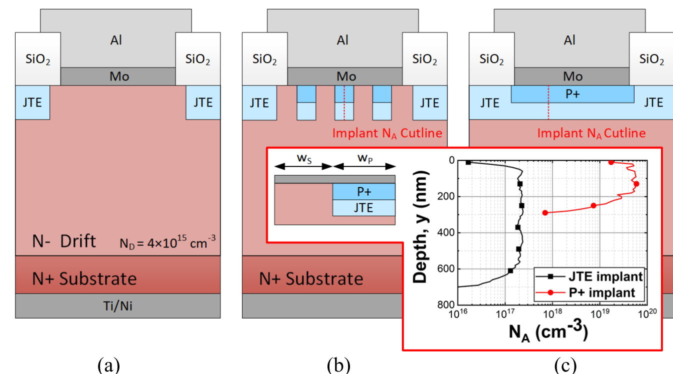

Fig. 1. Schematic of 4H-SiC (a) SBD, (b) JBS, and (c) p-i-n diode. Inset: the active area of the JBS diode, which uses a shallow, highly doped p$^+$-implant on top of the JTE implant, with w_S the Schottky width and w_P the p$^+$ implant width. Also shown are the JTE/p$^+$ doping profiles as they feature in the JBS and PiN diodes.

competitors for high-voltage power electronics applications. Due to its availability on large-diameter wafers (up to 150 mm), in combination with relatively low defect densities, silicon carbide (SiC)is the most widely developed wide bandgap semiconductor material [1]. Since the first SiC diodes were commercially available in 2001, Schottky barrier diodes (SBDs) and MOSFETs have penetrated the power device market and are now offered by a wide range of suppliers, providing faster switching, better thermal robustness, and increased efficiency when compared with their bipolar Si counterparts [2], [3]. In addition, the materials used for ultrahigh voltage applications ($\geq$3.3 kV) such as traction, static VAR compensation, and high-voltage direct current (HVDC) is the focus of extended research activities, where multiple unipolar and bipolar switches with blocking voltages up to and exceeding 20 kV have been successfully demonstrated [4].

Despite these developments in high-voltage switches, diodes in the voltage range up to 1700 V still represent the most mature and widely used SiC device. These most commonly feature implanted p$^+$ regions within a regular SBD's metal–semiconductor interface (see Fig. 1). These implants are used to shift the electric field peak away from the metal–semiconductor interface, lowering OFF-state leakage current [5], [6] and improving the surge current capabilities [7], [8], both being essential for high-voltage applications. In the merged PiN-Schottky (MPS) diode variant, the PiN regions in the active area turn on at voltages around 3 V, after

This work is licensed under a Creative Commons Attribution 4.0 License. For more information, see https://creativecommons.org/licenses/by/4.0/

the SBD regions have started conducting current at voltages close to the built-in potential (0.7–1.2 V). Hence, MPS devices offer the potential to increase the current-carrying capability compared with SBD planar Schottky devices [9] by carrier injection in the p^+ area. However, selecting a metal contact that forms both a good Schottky metal and a good p^+ ohmic contact is very difficult, and hence most SiC diodes are actually junction barrier Schottky (JBS) diodes, in which there is no hole injection from the p^+ regions.

The performance of a JBS or MPS power diodes is still predominantly governed by the choice of Schottky contact metal, which in turn determines the Schottky barrier height (SBH) at the metal–semiconductor interface. This selection determines the fundamental trade-off in performance between low ON-state voltage drop and low leakage current levels. Theoretical considerations of the exact conduction mechanisms in the ON-state and the OFF-state have also been widely investigated, with Tung's description of thermionic field emission dominating the conduction of Schottky diodes being the basis of most attempts to exactly model both leakage current levels and ON-state performance [10], [11]. Over the past decade, industrial suppliers have moved away from high work function metals such as nickel (Ni) toward lower work function metals such as titanium (Ti) [12], [13] and molybdenum [14], [15], where a decrease in forward voltage drop has come at the expense of higher leakage currents. More recently, molybdenum nitride (MoN) has been selected as metal by companies for their low barrier height devices [16], [17], which were demonstrated to have even lower barrier heights. Using refractory metals with low work functions or attempting to tune barrier heights by pre-conditioning the surface prior to metallization [13], [18]–[20], it has been shown that the performance of SBDs can be further improved by lowering the SBH.

In this investigation, we demonstrate a comprehensive study to optimize the use of the JBS technology for the 3.3 kV blocking voltage range by improving both the termination structure and the active area of the devices, offering a novel and industrially relevant approach to using the advantages of both bipolar and unipolar device action.

II. Device Structure and Fabrication

Fully terminated planar Schottky, JBS, and PiN diodes were fabricated. In the JBS and PiN diodes, the goal was to use the same implantations required for the termination structure as for the deep p-regions in the active area designed to reduce the electric field at the SiC surface.

The devices were made on a 4 × 10^{15} cm^{-3} nitrogen-doped, 35 μm thick 4H-SiC drift region, which was grown on highly n-doped substrates. Cross sections of the devices can be seen in Fig. 1, with the active area of the JBS diodes being shown in Fig. 1(d), with w_P the width of the p^+ implants (in μm) and w_S the width of the Schottky regions between the implants. The wafers were laser-cut into chips, before they were cleaned using a standard RCA 1/HF (10%)/RCA 2/HF (10%) process. In the active area, a shallow, highly doped aluminum (Al) implant (200 nm deep, 3 × 10^{19} cm^{-3} box profile doping) was carried out on top of a JTE implant (600 nm deep, 2 × 10^{17} cm^{-3} box profile doping). Implantation was carried out at 500 °C. After Al implantation, the samples underwent post-implantation activation at 1650 °C for 45 min and a sacrificial oxidation step at 1300 °C for 2 h in nitrous oxide ambient. A 2 μm thick SiO_2 field passivation layer was then LPCVD-deposited on the topside using a tetraethyl orthosilicate (TEOS) precursor. Ti (30 nm)/Ni (100 nm) ohmic contacts were then formed on the backside of the samples after a rapid thermal anneal at 1000 °C for 2 min in Ar (5 slm) ambient. In the next step, 100 nm thick Schottky contact metals (Mo, Ni, Ti) were deposited and then annealed at 500 °C for 2 min to form Schottky contact. Finally, a 4 μm thick polyimide layer was spun onto the surface and then patterned and etched before a 1.5–2 μm aluminum (Al) pad metal was deposited. This served as a field plate and to aid wire-bonding for switching tests.

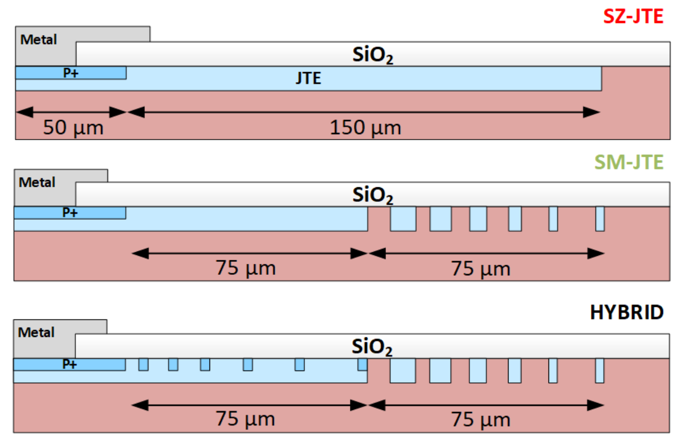

Fig. 2. Overview of the three different termination designs used in this investigation with (top) the single-zone JTE (SZJTE) design, (center) the space-modulated multiple-zone JTE (SM-JTE) termination, and (bottom) the (bottom) hybrid design. The hybrid termination consists of p^+ rings and multiple JTE rings. p^+ ring widths are fixed at 3 μm (3, 3, 4, 6, 8, 11 μm gaps). JTE ring widths are 14, 11, 7, 5, 4, and 3 μm (3, 3, 4, 5, 7, and 9 μm gaps).

To investigate the impact of different Schottky widths (w_S) and PiN widths (w_P) on the electrical characteristics, these parameters were varied in the investigation. The Schottky device splits are listed in Table I, while a full p-i-n diode was also made for comparison to these devices.

III. Termination Design Considerations

To optimize the OFF-state performance of the device, a range of termination designs were investigated, with their cross sections shown in Fig. 2. Here, a single zone junction termination extension (SZ-JTE) design, such as those used previously [21], [22], was used as a baseline. Also, a space-modulated JTE (SM-JTE) [23], [24] can be seen in Fig. 2 (central). Furthermore, a novel hybrid JTE design was used and is shown in Fig. 2 (bottom). The hybrid JTE comprises two zones, produced using a p^+ implant (200 nm depth, 3 × 10^{19} cm^{-3} box profile doping) and a single JTE implant (600 nm depth, variable box profile doping), both of which

TABLE I

OVERVIEW OF THE ON- AND OFF-STATE ELECTRICAL MEASUREMENTS OF THE JBS SCHOTTKY DIODES. DEVICE AREA IS 0.0156 cm^2

ID	Description	w_s/w_p (µm)	SBH (eV)			Ideality factor			I_L at 3300 V (µA)			Breakdown Voltage (V)		
			Mo	Ni	Ti	Mo	Ni	Ti	Mo	Ni	Ti	Mo	Ni	Ti
1	Benchmark	3/3	1.16	1.67	1.31	1.01	1.02	1.03	190	700	0.035	3466	3411	3465
2	Wide Features	4/4	1.15	1.62	0.88	1.01	1.05	1.01	-	25	250	1831	3488	3583
3	Narrow Features	2/2	1.17	1.68	1.62*	1.01	1.02	1.38*	0.60	0.10	1.45	3560	3520	3465
4	Narrow w_s	2/3	1.07*	1.69	1.37*	1.28*	1.02	1.56*	-	0.17	6.5	2345	3501	3560
5	Wide w_s	4/3	1.15	1.66	1.28	1.01	1.03	1.04	150	0.13	-	3464	3600	-
6	Wide w_p	3/4	1.18	1.67	1.38	1.01	1.03	1.01	60	0.90	0.015	3325	3600	3500
7	Narrow w_s/wide w_p	2/4	1.10*	1.71	2.71*	1.26*	1.02	6.21*	0.30	0.11	0.75	3430	3481	3580
8	Full Schottky	1/0	1.11	1.61	0.87	1.02	1.03	1.07	-	30	-	885	3662	-

*Results skewed by poor I-V characteristics, potentially due to the pinching of the narrow Schottky regions.

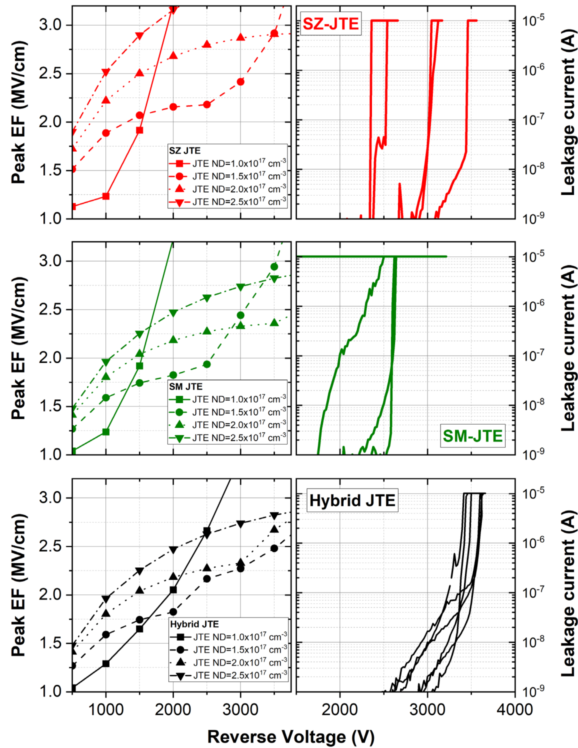

Fig. 3. Left: results of peak electric field (Peak EF) simulations of the SZ, SM, and hybrid JTE designs, each including four different JTE doping values from 1×10^{17} to 2.5×10^{17} cm^{-3}. Right: results of breakdown measurements for the corresponding JTEs as implemented on fabricated p-i-n diodes for a JTE box profile doping concentration of 2×10^{17} cm^{-3}.

are Al^+ implants carried out at 500 °C. In the first innermost zone (75 μm total width), space-modulated p^+ floating rings are implanted into the JTE region that extends from the active region. A second zone, outside of the first, features the space modulation of the JTE implant itself in multiple floating JTE rings (75 μm total width). These two implants were also used to form the P region(s) in the active area, as shown in Fig. 1.

To optimize the performance of the different termination designs, peak electric field (EF) simulations were carried out at voltage biases from 500 to 5000 V. These were used to simulate the maximum EF reached for each JTE box profile doping value from 1×10^{17} to 2.5×10^{17} cm^{-3} at 150 °C. A first overview of the results of these simulations can be seen in Fig. 3. The results revealed that the SM-JTE, with a doping concentration of 2×10^{17} cm^{-3}, reached the highest voltage, or 4000 V before reaching a peak EF of 2.5×10^6 V/cm. This was compared with 3000 V for the SZ-JTE and 3500 V for the hybrid design, both at 1.5×10^{17} cm^{-3}. Despite the slightly lower voltage possible, the hybrid JTE design shows greater immunity to doping variations, hence offering a greater possibility of reaching high breakdown voltages for real devices, where the implantation dose has an associated margin of error. All three of the termination designs were taken forward to the p-i-n diode fabrication phase and, to allow for process deviations, a 2×10^{17} box profile doping concentration was chosen for the different JTE regions. For the hybrid termination design, p^+ doping was chosen to be 3×10^{19} cm^{-3} to assist with both the potential formation of an ohmic contact when selecting an appropriate metal stack with sufficiently low specific contact resistivity and a sufficiently low implant dose to help with re-crystallization during the post-implantation anneal [25].

The results of breakdown measurements on p-i-n diodes which utilized these different termination designs are depicted in Fig. 3 (right). Both the SZ-JTE and hybrid devices comfortably exceed the desired blocking voltage of 3300 V, confirming the successful activation of p-dopants, with the hybrid devices showing a much tighter distribution with no device reaching a leakage current level of 1×10^{-7} A below 3000 V. However, all SZ-JTE devices broke down before reaching blocking voltages of 2600 V. This suggests that the activated P concentration in the JTE may have fallen outside of the very narrow processing window that was required to optimize the SZ-JTE.

In this section, we used p-i-n diodes to demonstrate the applicability of the hybrid termination design for 3.3 kV devices and benchmarked it against widely used commercial termination design structures. In the next step, the JBS diodes were fabricated using the hybrid JTE design, and their ON- and OFF-state characteristics were extracted.

IV. ELECTRICAL RESULTS OF THE OPTIMIZED SCHOTTKY DEVICES

The 3.3 kV JBS diodes used Mo, Ti, and Ni as Schottky contact metals, with each chip containing the eight device types

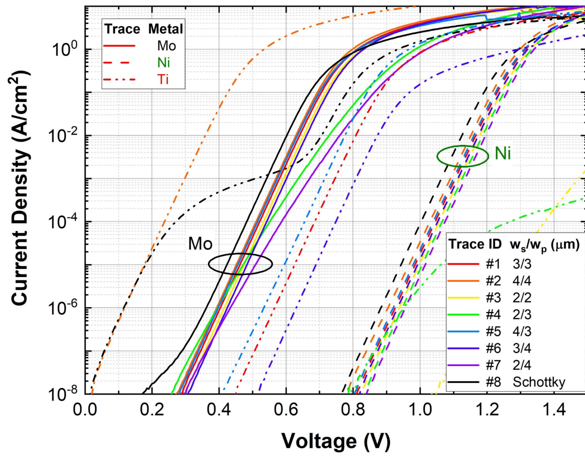

Fig. 4. Overview of the ON-state of the fully terminated Mo, Ti, and Ni JBS diodes. The full active area is 0.0156 A.cm^2; the Schottky area through which current flows is A.w$_s$/(w$_s$ + w$_p$).

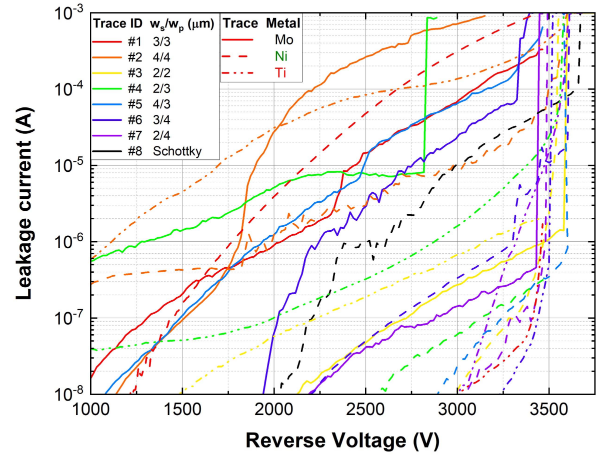

Fig. 5. Overview of selected breakdown measurements up to 4000 V on the fully terminated Mo, Ti, and Ni JBS diodes. Device area is 0.0156 A.cm^2.

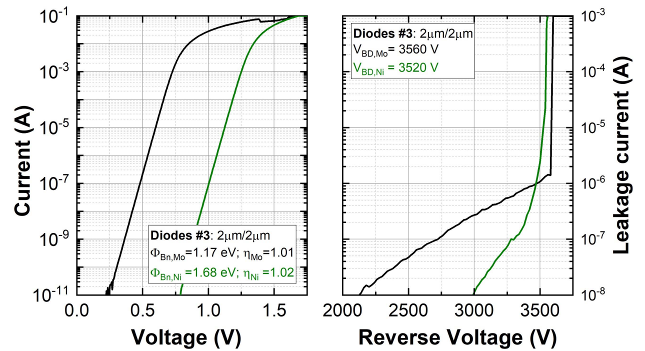

Fig. 6. ON- and OFF-state responses of the Ni and Mo Schottky diodes with a w$_s$/w$_p$ ratio of 2:2 μm.

as listed in Table I. The ON-state characteristics of diodes with an active area (A) of 1.56 mm^2 can be seen in Fig. 4. These were obtained via an auto-prober at room temperature using a Keysight B1505A parameter analyzer with a Semiprobe semi-automatic probe station. Their ON-state parameters, ideality factor (η), and SBH are listed in Table I. These were extracted in the current density range of 1×10^{-7}–1×10^{-2} A.cm^{-2}, following the thermionic emission theory which can be found in [10] and [11]. The Schottky-only area (A.w$_s$/[w$_s$ + w$_p$]) was used rather than the full active area (A) in plotting Fig. 4 and in extracting these data. The majority of the devices, and all the Ni diodes investigated, had extremely low values of η, confirming the assumption that thermionic emission is the dominant conduction mechanism at the interface. The SBHs extracted for the three metals correlate well with previous reports [15], [26], the Ni offering a very high barrier at 1.6 eV, the Mo 1.1 eV, and the Ti as low as 0.87 eV in the best case. While interfacial formation of silicides or carbides in Mo has been shown to be very unlikely [15], the partial formation of these at 500 °C is possible in Ni [27] and Ti [28]–[30] SiC SBDs and could be related to the inhomogeneity in the Ti systems while being the source of reliable Ni Schottky contacts [27]. The impact of width changes in the Schottky region and the p$^+$-implanted region on the contact resistance and surge current behavior have not been investigated and are beyond the scope of this investigation.

Following ON-state measurements, the reverse characteristics of the same 3.3 kV chips were assessed. To prevent arcing during measurements, samples were covered in fluorinert oil. Fig. 5 shows the characteristics of all the 1.56 mm^2 JBS diodes, and in Table I the leakage current (I_L) at 3.3 kV and the breakdown voltage of the devices are listed. Furthermore, validating the hybrid termination design, the breakdown voltage of the majority of the devices exceeded the target voltage of 3.3 kV without premature breakdown, irrespective of their choice of Schottky contact metal. Furthermore, leakage currents (I_L) exceeded a current level of 1×10^{-5} A only at voltages higher than 3 kV for the majority of the devices presented.

Special attention is drawn to design 3, as shown in Fig. 6 for the Ni and Mo devices. As one of the three designs with a 50:50 Schottky:PiN ratio, this design has the narrowest pitch with the p$^+$ implants/Schottky regions being 2 μm wide. As a result, these devices have exemplary OFF-state performance, while the 50% Schottky ratio allows for a high-quality turn-on with relatively low forward voltage drop. These are perhaps the best balanced diodes of those presented.

Fig. 7 shows the $I - V$ characteristics of the Mo and Ni planar Schottky devices which were taken up to their rated current of 2 A, with values of specific ON-resistance ($R_{\text{ON,SP}}$) of 15 and 15.5 mΩ.cm^2, respectively. These are compared with a p-i-n diode which used a Ti/Al (30/100 nm) topside metal stack which was annealed at 1000 °C to create an ohmic contact. This bipolar device showed a typical PiN response, turning on at approximately 2.7 V, but with a slightly reduced $R_{\text{ON,SP}}$ of 11.9 mΩ.cm^2. While this is about 4 mΩ.cm^2 lower than the other devices, a lifetime enhancement process [31] would boost conductivity modulation and reduce this further. Despite this, $R_{\text{ON,SP}}$ agrees with the already reported values for similar SiC unipolar power diodes [21]. This result was validated across several chips and wafers.

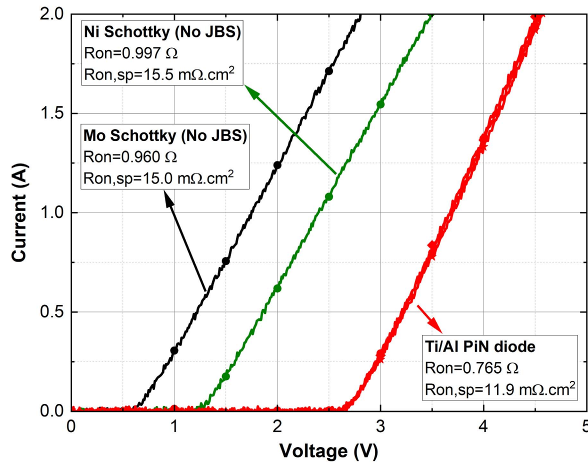

Fig. 7. Exemplary ON-state results of Ni and Mo planar Schottky diodes and a Ti/Al PiN diode which was fabricated on the same chip, which were rated up to 2 A, and their respective specific ON-resistance, $R_{ON,SP}$ (mΩ.cm^2). Device area is 0.0156 cm^2.

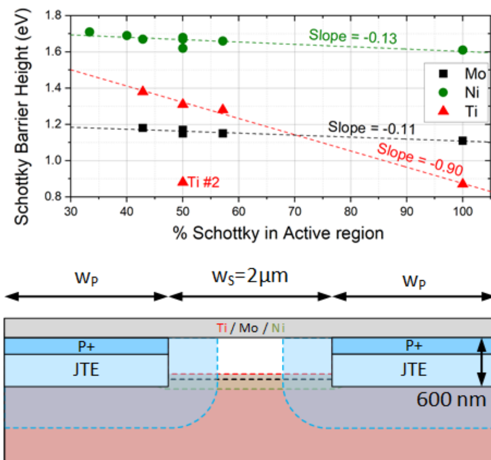

Fig. 8. (Top) SBH of the diodes plotted versus their percentage Schottky coverage. (Bottom) a to-scale representation of a JBS diode with w_s = 2 μm, with calculated 0 V depletion regions appended.

V. Discussion and Trends

Common trends appear within the ON- and OFF-state results. Despite reducing the area in the thermionic emission equation to eliminate the implanted regions of p$^+$, all three datasets display a correlation between the Schottky coverage and the SBH, as plotted in Fig. 8. The full Schottky diodes have the lowest SBH in each of the three datasets and as the p$^+$ coverage increases, so too does the SBH. The reason for this trend is due to the depletion region that surrounds the p$^+$ regions, which according to standard depletion region calculations [32] extends 570 nm into the Schottky region at 0 V, reducing the Schottky area—as shown to scale in Fig. 8. To those devices with the narrowest Schottky 2 μm openings, this is a pinching JFET-like effect across more than half of the Schottky opening. Several of the devices, marked in Table I, with 2 μm Schottky openings and wider PiN regions from this dataset were evidently skewed in Fig. 4 as a result of this.

What is also of interest from this dataset is while a good linear fit is possible to all the non-pinched-off data, as shown in Fig. 8, very different slopes were achieved. This is potentially attributable to the differing depletion region widths that form from the Schottky interface, which are again shown to scale in Fig. 4 using standard calculations [32]. With the 600 nm deep JTE implants used in this region, only the 630 nm deep depletion region resulting from the 1.61 eV Ni SBH depletes the bottom of the JTE implant, thereby reshaping/engineering the depletion profile and reducing the pinching effect. Conversely, the Ti contacts with a 0.87 eV SBH has a 0 V depletion region of 440 nm, falling short of the JTE depth. Consequently, it is proposed that this pinching beneath the Schottky depletion region explains the greater SBH fluctuation and the three devices with poor $I - V$ characteristics.

In this study, the p-regions in the active area are relatively deep, at 600 nm, as they use the same implants as the termination region. While this depth benefits the OFF-state and is fine for the Ni diodes, it is clear that this a further step in optimizing the Ti, and possibly also the Mo diodes would be to reduce the implant depth to 400 nm or less.

It is of little surprise that p$^+$ pinching has a positive impact on the OFF-state results. The devices skewed by pinching in the ON-state generally get the benefit of low leakage in the OFF-state. Across the dataset, the designs with the narrowest Schottky regions and the smallest Schottky percentage are the diodes with the lowest OFF-state leakage at the rated voltage of 3.3 kV. These designs are effective at shifting the peak of the electric field down, away from the Schottky interface to the bottom of the implanted p-regions. With a reduced electric field at the surface, the leakage due to tunneling is greatly reduced.

For completeness, Ti device #2, marked in Fig. 8, fell outside of the trend described, with an excellent low SBH ON-state, but an OFF-state with high leakage. This is explainable as it has wide 4 μm features, and hence pinching has little effect, and the device behave similar to a full Ti Schottky.

VI. Conclusion

The 3.3 kV JBS diodes have been successfully developed that feature a validated hybrid JTE design, the implants for which are also used in the device's active region. Diodes made from Ni and Mo, which feature 2 μm wide Schottky and PiN regions, display excellent characteristics in both the ON- and OFF-state. These diodes and the majority of the other designs display near-ideal characteristics, while the leakage remains very low until they breakdown at $>$3500 V. Several diodes were also shown to work to the rated current of 2 A. Devices made using Ti are shown to be affected most adversely from JFET pinching effects, most likely due to the shallow depletion region that forms compared with the p-type implant depth.

References

[1] T. Kimoto and Y. Yonezawa, "Current status and perspectives of ultrahigh-voltage SiC power devices," *Mater. Sci. Semicond. Process.*, vol. 78, pp. 43–56, May 2018, doi: 10.1016/j.mssp.2017.10.010.

[2] X. She, A. Q. Huang, O. Lucia, and B. Ozpineci, "Review of silicon carbide power devices and their applications," *IEEE Trans. Ind. Electron.*, vol. 64, no. 10, pp. 8193–8205, Oct. 2017, doi: 10.1109/TIE.2017.2652401.

[3] S. Ji, Z. Zhang, and F. Wang, "Overview of high voltage SiC power semiconductor devices: Development and application," *CES Trans. Elect. Mach. Syst.*, vol. 1, no. 3, pp. 254–264, Sep. 2017, doi: 10.23919/TEMS.2017.8086104.

[4] E. Van Brunt, L. Cheng, M. J. O'Loughlin, J. Richmond, V. Pala, J. W. Palmour, C. W. Tipton, and C. Scozzie, "27 kV, 20 A 4H-SiC n-IGBTs," *Mater. Sci. Forum*, vol. 821, pp. 847–850, Jun. 2015, doi: 10.4028/www.scientific.net/msf.821-823.847.

[5] C. Bodeker, T. Vogt, and N. Kaminski, "Stability of silicon carbide Schottky diodes against leakage current thermal runaway," in *Proc. IEEE 27th Int. Symp. Power Semiconductor Devices IC's (ISPSD)*, May 2015, pp. 245–248, doi: 10.1109/ISPSD.2015.7123435.

[6] L. Di Benedetto, G. D. Licciardo, T. Erlbacher, A. J. Bauer, and S. Bellone, "Analytical model and design of 4H-SiC planar and trenched JBS diodes," *IEEE Trans. Electron Devices*, vol. 63, no. 6, pp. 2474–2481, Jun. 2016, doi: 10.1109/TED.2016.2549599.

[7] J. Wu, N. Ren, H. Wang, and K. Sheng, "1.2-kV 4H-SiC merged PiN Schottky diode with improved surge current capability," *IEEE J. Emerg. Sel. Topics Power Electron.*, vol. 7, no. 3, pp. 1496–1504, Sep. 2019, doi: 10.1109/JESTPE.2019.2921970.

[8] S. Palanisamy, S. Fichtner, J. Lutz, T. Basler, and R. Rupp, "Various structures of 1200 V SiC MPS diode models and their simulated surge current behavior in comparison to measurement," in *Proc. 28th Int. Symp. Power Semiconductor Devices ICs (ISPSD)*, Jun. 2016, pp. 235–238, doi: 10.1109/ISPSD.2016.7520821.

[9] H. Niwa, J. Suda, and T. Kimoto, "Ultrahigh-voltage SiC MPS diodes with hybrid unipolar/bipolar operation," *IEEE Trans. Electron Devices*, vol. 64, no. 3, pp. 874–881, Mar. 2017, doi: 10.1109/TED.2016.2636573.

[10] R. T. Tung, "Electron transport at metal-semiconductor interfaces: General theory," *Phys. Rev. B, Condens. Matter*, vol. 45, no. 23, 1992, Art. no. 013509, doi: 10.1103/PhysRevB.45.13509.

[11] P. M. Gammon *et al.*, "Modelling the inhomogeneous SiC Schottky interface," *J. Appl. Phys.*, vol. 114, no. 22, Dec. 2013, Art. no. 223704, doi: 10.1063/1.4842096.

[12] F. Roccaforte, G. Brezeanu, P. Gammon, F. Giannazzo, S. Rascunà, and M. Saggio, "Schottky contacts to silicon carbide: Physics, technology and applications," in *Advancing Silicon Carbide Electronics Technology, I: Metal Contacts to Silicon Carbide: Physics, Technology, Applications*. 2018, doi: 10.21741/9781945291852-3.

[13] G. Bellocchi *et al.*, "Barrier height tuning in Ti/4H-SiC Schottky diodes," *Solid-State Electron.*, vol. 186, Dec. 2021, Art. no. 108042, doi: 10.1016/j.sse.2021.108042.

[14] T. Zhang, C. Raynaud, and D. Planson, "Measure and analysis of 4H-SiC Schottky barrier height with mo contacts," *Eur. Phys. J. Appl. Phys.*, vol. 85, no. 1, p. 10102, Jan. 2019, doi: 10.1051/epjap/2018180282.

[15] A. B. Renz *et al.*, "The improvement of Mo/4H-SiC Schottky diodes via a P_2O_5 surface passivation treatment," *J. Appl. Phys.*, vol. 127, no. 2, Jan. 2020, Art. no. 025704, doi: 10.1063/1.5133739.

[16] Infineon Technologies AG. *CoolSiC Schottky Diode 650V G5 and G6, Improved Efficiency and Price Performance*. Accessed: Sep. 18, 2021. [Online]. Available: https://www.infineon.com/cms/en/product/power/silicon-carbide-sic/coolsic-schottky-diode/coolsic-schottky-diode-650v-g5-and-g6/#G6

[17] L. Stöber, J. Konrath, F. Patocka, M. Schneider, and U. Schmid, "Controlling 4H–SiC Schottky barriers by molybdenum and molybdenum nitride as contact materials," *IEEE Trans. Electron Devices*, vol. 63, no. 2, pp. 578–583, Feb. 2016, doi: 10.1109/TED.2015.2504604.

[18] V. E. Gora *et al.*, "Comparison of nickel, cobalt, palladium, and tungsten Schottky contacts on n-4H-silicon carbide," *Phys. B, Condens. Matter*, vol. 535, pp. 333–337, Apr. 2018, doi: 10.1016/j.physb.2017.08.024.

[19] M. Vivona *et al.*, "Electrical properties of inhomogeneous tungsten carbide Schottky barrier on 4H-SiC," *J. Phys. D, Appl. Phys.*, vol. 54, no. 5, Feb. 2021, Art. no. 055101, doi: 10.1088/1361-6463/abbd65.

[20] L. Knoll, V. Teodorescu, and R. A. Minamisawa, "Ultra-thin epitaxial tungsten carbide Schottky contacts in 4H-SiC," *IEEE Electron Device Lett.*, vol. 37, no. 10, pp. 1318–1320, Oct. 2016, doi: 10.1109/LED.2016.2604488.

[21] Y. Pan, L. Tian, H. Wu, Y. Li, and F. Yang, "3.3 kV 4H-SiC JBS diodes with single-zone JTE termination," *Microelectron. Eng.*, vol. 181, pp. 10–15, Sep. 2017, doi: 10.1016/j.mee.2017.05.054.

[22] K. Vassilevski *et al.*, "High voltage silicon carbide Schottky diodes with single zone junction termination extension," *Mater. Sci. Forum*, vols. 556–557, pp. 873–876, Sep. 2007, doi: 10.4028/www.scientific.net/msf.556-557.873.

[23] H. Bartolf, V. Sundaramoorthy, A. Mihaila, M. Berthou, P. Godignon, and J. Millan, "Study of 4H-SiC Schottky diode designs for 3.3 kV applications," *Mater. Sci. Forum*, vol. 778, pp. 795–799, Jan. 2014, doi: 10.4028/www.scientific.net/msf.778-780.795.

[24] H. Niwa, G. Feng, J. Suda, and T. Kimoto, "Breakdown characteristics of 15-kV-class 4H-SiC PiN diodes with various junction termination structures," *IEEE Trans. Electron Devices*, vol. 59, no. 10, pp. 2748–2752, Oct. 2012, doi: 10.1109/TED.2012.2210044.

[25] T. Kimoto and J. A. Cooper, *Fundamentals of Silicon Carbide Technology: Growth, Characterization, Devices and Applications*. Hoboken, NJ, USA: Wiley, 2014, doi: 10.1002/9781118313534.

[26] A. B. Renz *et al.*, "Surface effects of passivation within Mo/4H-SiC Schottky diodes through MOS analysis," *Mater. Sci. Forum*, vol. 963, pp. 511–515, Jul. 2019, doi: 10.4028/www.scientific.net/msf.963.511.

[27] F. Roccaforte, F. La Via, V. Raineri, P. Musumeci, L. Calcagno, and G. G. Condorelli, "Highly reproducible ideal SiC Schottky rectifiers: Effects of surface preparation and thermal annealing on the Ni/6H-SiC barrier height," *Appl. Phys. A, Solids Surf.*, vol. 77, no. 6, pp. 827–833, Nov. 2003, doi: 10.1007/s00339-002-1981-8.

[28] S. Kyoung, E.-S. Jung, and M. Y. Sung, "Post-annealing processes to improve inhomogeneity of Schottky barrier height in Ti/Al 4H-SiC Schottky barrier diode," *Microelectron. Eng.*, vol. 154, pp. 69–73, Mar. 2016, doi: 10.1016/j.mee.2016.01.013.

[29] H. Lin-Chao *et al.*, "Annealing temperature influence on the degree of inhomogeneity of the Schottky barrier in Ti/4H—SiC contacts," *Chin. Phys. B*, vol. 23, no. 12, 2014, Art. no. 127302, doi: 10.1088/1674-1056/23/12/127302.

[30] Q.-W. Song, Y.-M. Zhang, Y.-M. Zhang, F.-P. Chen, and X.-Y. Tang, "Investigation of current transport parameters of Ti/4H-SiC MPS diode with inhomogeneous barrier," *Chin. Phys. B*, vol. 20, no. 5, May 2011, Art. no. 057301, doi: 10.1088/1674-1056/20/5/057301.

[31] T. Kimoto *et al.*, "Carrier lifetime and breakdown phenomena in SiC power device material," *J. Phys. D: Appl. Phys.*, vol. 51, no. 36, Sep. 2018, Art. no. 363001, doi: 10.1088/1361-6463/aad26a.

[32] S. M. Sze, Y. Li, and K. K. Ng, *Physics of Semiconductor Devices*. Hoboken, NJ, USA: Wiley, 2021, doi: 10.1002/0470068329.